

Mössbauer Emission Spectra of ^{119}Sn in Binary Compounds of Antimony and Tellurium

Shizuko Ambe* and Fumitoshi Ambe

The Institute of Physical and Chemical Research (RIKEN), Wako, Saitama 351-01

(Received December 19, 1994)

The Mössbauer emission spectra of defect ^{119}Sn atoms arising from ^{119}Sb and $^{119\text{m}}\text{Te}$ were measured in GaSb, InSb, In_2Te_3 , ZnSb, CdSb, CdTe, and Ag_2Te . The lattice sites of defect ^{119}Sn atoms in these binary compounds were determined on the basis of the obtained Mössbauer parameters and the recoil energy associated with EC decays of the source nuclides. Together with the results of previous studies, the isomer shifts of both defect and normal ^{119}Sn were shown to correlate with the electronegativity of ligands in binary compounds of the main-group elements, such as Sn, Sb, and Te.

The electronic state of defect atoms produced by nuclear decays and reactions can be studied in a time range on the order of 100 ns or less by Mössbauer emission spectroscopy.¹⁾ Defect atoms often exist in an unusual chemical state which cannot be formed by synthetic chemical techniques. We have been studying the chemical states of ^{119}Sn atoms arising from electron-capture (EC) decays of ^{119}Sb and $^{119\text{m}}\text{Te}$ (Fig. 1) which were chemically doped in various matrices or deposited on different solid surfaces.^{2–9)} It was demonstrated that the isomer shifts of defect and normal ^{119}Sn in a series of binary compounds of the main-group elements, such as Sn, Sb, and Te, are determined to a first approximation by the electronegativity of their nearest-neighbor atoms (here, 'normal ^{119}Sn ' denotes ^{119}Sn atoms occupying Sn sites of the compounds).^{2–4)} Little is known about the electronic states of tin bonded to ligand atoms having atomic numbers smaller than that of tin.

Extensive Mössbauer studies have been carried out on radioactive ions implanted in a variety of

matrices.^{10–14)} In this type of experiment, well-characterized matrices prepared beforehand can be employed. However, extra atoms are brought into the matrix, which may disturb the local environment of probe atoms during the measurement. In fact, Mössbauer spectra obtained after implanting source nuclides often consist of lines ascribable not only to a substitutional site, but also to interstitial sites, vacancy-associated defect structures, and even defect structures containing oxygen atoms.¹⁵⁾ Moreover, high-dose implantation makes the spectra more complex by forming new phases in the matrix.¹⁶⁾

On the other hand, a chemical doping method requires the preparation of samples containing radioactive nuclides in small amounts and in limited time; their characterization is often restricted because of their radioactivity. However, this method has merit in that the local environment of defect atoms is affected only by the nuclear decay.

In the present work our Mössbauer emission studies by a chemical-doping technique were extended to matrices, which were expected to give defect ^{119}Sn atoms having indium, cadmium and silver as the nearest-neighbor atoms. The lattice sites of defect ^{119}Sn atoms produced by the EC decays of ^{119}Sb and $^{119\text{m}}\text{Te}$ in the matrices were determined on the basis of the observed Mössbauer parameters as well as a consideration of the chemical nature of the elements involved and the recoil energy of EC decays. Together with the results of previous studies, the isomer shifts of both defect and normal ^{119}Sn were shown to correlate with the electronegativity of the ligands from silver to iodine.

Experimental

Materials. The source nuclide $^{119\text{m}}\text{Te}$ (half-life: 4.68 d) was produced by α -irradiation of metallic tin using the

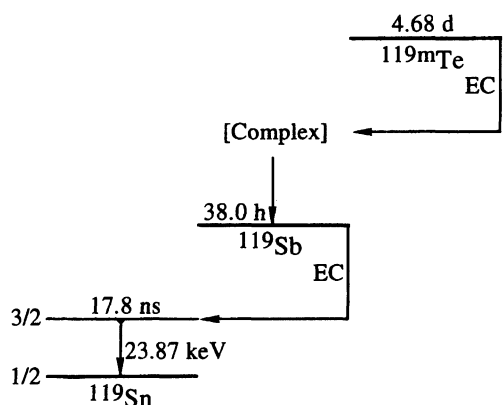


Fig. 1. Simplified decay scheme of ^{119}Sb and $^{119\text{m}}\text{Te}$.

Riken 160 cm cyclotron, while ^{119}Sb (half-life: 38.0 h) was obtained by milking from $^{119\text{m}}\text{Te}$. Radiochemical procedures for separating the nuclides and preparing ^{119}Sb and $^{119\text{m}}\text{Te}$ metals as starting materials have been described in previous papers.^{2,4)} Antimony metal containing carrier-free $^{119\text{m}}\text{Te}$ was obtained from a 6 mol dm⁻³ HCl solution of Sb^{3+} and carrier-free $^{119\text{m}}\text{Te}^{4+}$ ions by reducing with a Cr^{2+} solution, and was purified by sublimation in vacuum. Ga^{119}Sb , In^{119}Sb , InSb doped with carrier-free $^{119\text{m}}\text{Te}$ [designated hereafter as $\text{InSb}(^{119\text{m}}\text{Te})$], $\text{In}_2^{119\text{m}}\text{Te}_3$, Zn^{119}Sb , Cd^{119}Sb , $\text{Cd}^{119\text{m}}\text{Te}$, and $\text{Ag}_2^{119\text{m}}\text{Te}$ were prepared by fusing stoichiometric mixture of the metals under argon. Nonstoichiometric samples with nominal compositions of $\text{In}^{119}\text{Sb}_{0.93}$ and $\text{In}^{119}\text{Sb}_{1.03}$ were similarly prepared.

The identity of the samples was verified by the powder X-ray patterns of similarly prepared cold samples. The Cd^{119}Sb sample was found to contain a small amount of Cd_3Sb_4 phase, probably due to the loss of a part of the Cd by evaporation during fusion. The other stoichiometric samples were found to be single phases.

Measurement. The Mössbauer emission spectra of the samples were measured at 78 K against a BaSnO_3 absorber (0.9 mg $^{119}\text{Sn}/\text{cm}^2$), also kept at 78 K. The samples labeled with $^{119\text{m}}\text{Te}$ were maintained at 78 K before the Mössbauer measurement until $^{119\text{m}}\text{Te}$ attained radioactive equilibrium with its daughter ^{119}Sb , so that the contribution of ^{119}Sb arising from $^{119\text{m}}\text{Te}$ before and during the sample preparation would be negligible. The obtained spectra were processed on FACOM M series computers installed at Riken.

Results

Typical Mössbauer emission spectra obtained are shown in Figs. 2, 3, 4, and 5 along with the results of fitting with Lorentzian lines. The spectra of the Ga^{119}Sb and In^{119}Sb samples comprise a single emission line at 1.86 and 1.94 mm s⁻¹ relative to BaSnO_3 , respectively (Figs. 2(a) and 2(b)). The sample with a nominal composition of $\text{In}^{119}\text{Sb}_{0.97}$ gave a single emission line at 1.96 mm s⁻¹, while the spectrum of $\text{In}^{119}\text{Sb}_{1.03}$ was slightly asymmetric and decomposable into a dominant line at 1.97 mm s⁻¹ and a subsidiary one fixed at 2.68 mm s⁻¹ (the isomer shift of ^{119}Sn in Sb metal²⁾) with an intensity ratio of roughly 1 to 0.03. (Fitting with a free position for the subsidiary line did not converge.) The $\text{InSb}(^{119\text{m}}\text{Te})$ sample gave an emission spectrum, which was decomposed into two Lorentzian lines. The dominant line has a center position of 1.88 mm s⁻¹ and the subsidiary one at 2.3 mm s⁻¹ with relative areas of 77 and 23%, respectively (Fig. 2(c)). The $\text{In}_2^{119\text{m}}\text{Te}_3$ sample gave a broad emission line with a shoulder, as shown in Fig. 2(d). Fitting with Lorentzian lines resulted in a singlet at 3.21 mm s⁻¹ along with a doublet (assumed to be symmetric) with a center position of 1.6 mm s⁻¹ and a splitting of 1.5 mm s⁻¹. The relative area of the singlet was 78%, and that of the doublet 22%. The emission spectra of Zn^{119}Sb and Cd^{119}Sb are shown in Figs. 3(a) and 3(b), respectively. They were both decomposed into two Lorentzians with almost the same line widths at 1.37 and 2.73 mm s⁻¹ for ZnSb and at

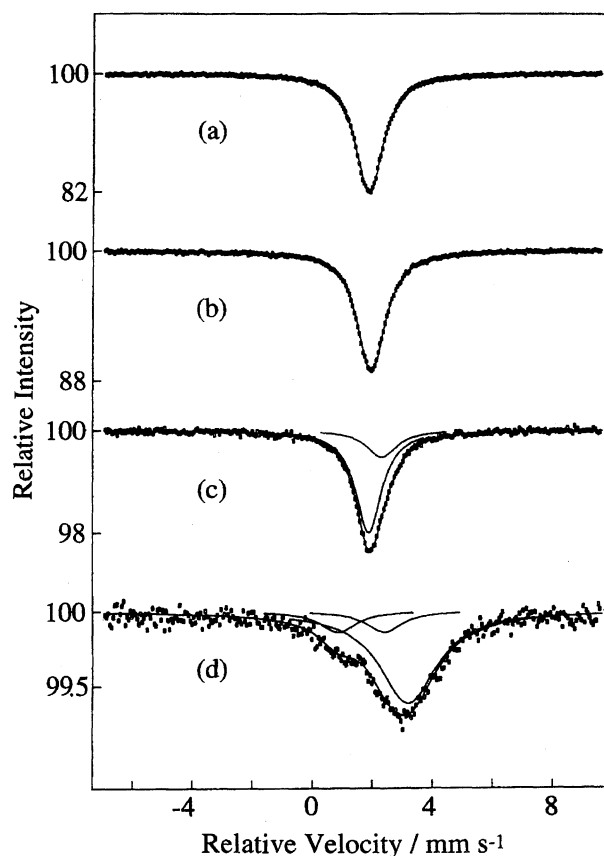


Fig. 2. Mössbauer emission spectra of ^{119}Sn arising from ^{119}Sb or from $^{119\text{m}}\text{Te}$ via ^{119}Sb in (a) Ga^{119}Sb , (b) In^{119}Sb , (c) $\text{InSb}(^{119\text{m}}\text{Te})$, and (d) $\text{In}_2^{119\text{m}}\text{Te}_3$ at 78 K.

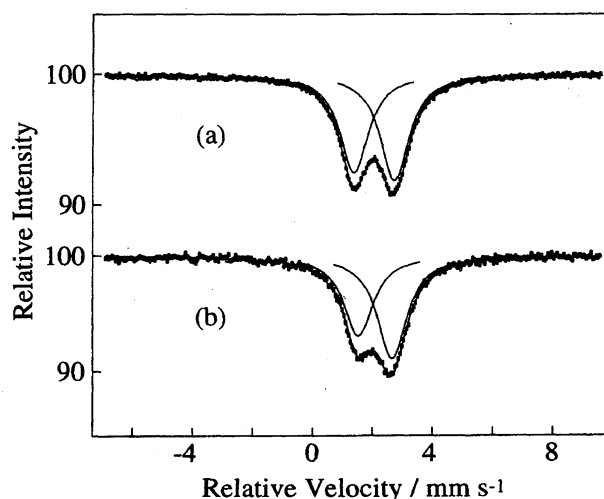


Fig. 3. Mössbauer emission spectra of ^{119}Sn arising from ^{119}Sb in (a) Zn^{119}Sb and (b) Cd^{119}Sb at 78 K.

1.53 and 2.66 mm s⁻¹ for CdSb . The $\text{Cd}^{119\text{m}}\text{Te}$ sample showed a broad emission line, which was decomposable into two Lorentzian lines with center positions of 1.95 and 2.76 mm s⁻¹, as shown in Fig. 4. The emission spectrum of $\text{Ag}_2^{119\text{m}}\text{Te}$ comprised two lines with essentially the same intensity and width at 1.09 and 3.41 mm s⁻¹

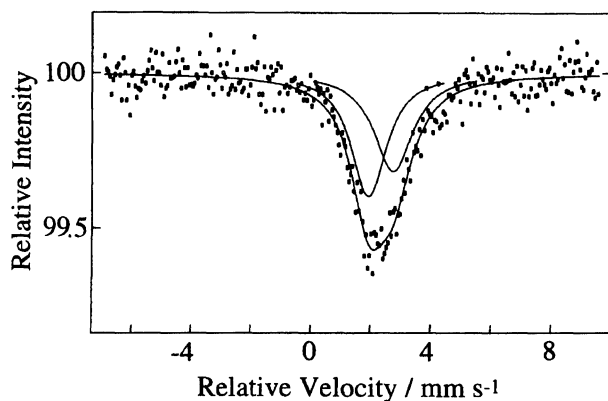


Fig. 4. Mössbauer emission spectra of ^{119}Sn arising from $^{119\text{m}}\text{Te}$ via ^{119}Sb in $\text{Cd}^{119\text{m}}\text{Te}$ at 78 K.

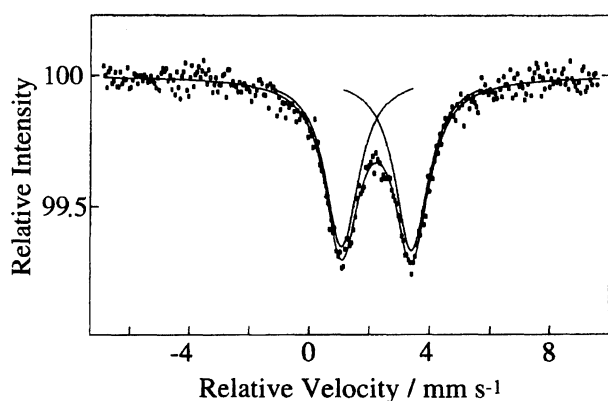


Fig. 5. Mössbauer emission spectra of ^{119}Sn arising from $^{119\text{m}}\text{Te}$ via ^{119}Sb in $\text{Ag}_2^{119\text{m}}\text{Te}$ at 78 K.

(Fig. 5).

The Mössbauer parameters of the emission lines based on the discussion described below are summarized in Table 1.

Discussion

Atomic Displacement by Recoil. The nuclear-decay series studied in the present work is $^{119\text{m}}\text{Te}$ (4.68 d) \rightarrow ^{119}Sb (38.0 h) \rightarrow $^{119}\text{Sn}^*$ (17.8 ns) \rightarrow ^{119}Sn , where $^{119}\text{Sn}^*$ denotes ^{119}Sn nuclei in the nuclear first excited level (Mössbauer level) of ^{119}Sn , as shown in Fig. 1. Since the recoil energy accompanying the EC decay of ^{119}Sb is estimated to be at most 1.5 eV, which is far smaller than the displacement energy in a solid, the daughter nuclide ^{119}Sn is considered to remain at the original site of ^{119}Sb unless it is chemically unfavorable for a tin atom. In the case of the EC decay of $^{119\text{m}}\text{Te}$ to ^{119}Sb , the recoil energy due to the neutrino emission is 24 eV, and that due to associated γ -rays has a maximum of 25 eV. Since the directions of recoil by these two mechanisms are uncorrelated, the eventual recoil energy is estimated to have a distribution beyond the displacement energy. In fact, it was demonstrated in our previous work⁴⁾ that ^{119}Sn atoms arising from ^{119}Sb in Sn^{119}Sb remain at the Sb site, while ^{119}Sn

atoms arising from $^{119\text{m}}\text{Te}$ via ^{119}Sb in $\text{Sn}^{119\text{m}}\text{Te}$ occupy both Sn and Te sites, the latter being dominant. These facts provide a basis for a site assignment of the defect atoms produced by nuclear decays in the present work.

The relative intensity of the emission lines of the samples with $^{119\text{m}}\text{Te}$ is much smaller than that of the emission lines of those with ^{119}Sb (Figs. 2, 3, 4, and 5). One reason is that the signal-to-noise ratio was much lower in measurements of $^{119\text{m}}\text{Te}$ sources, because the source nuclide emits many γ rays, causing a serious Compton background at 23.87 keV. On the other hand, ^{119}Sb emits only Mössbauer γ rays. Another probable reason is a reduction of the recoilless fraction due to some disturbance of the lattice around ^{119}Sn atoms due to recoil accompanying the EC decay of $^{119\text{m}}\text{Te}$.

Ga ^{119}Sb and In ^{119}Sb . GaSb and InSb have the zinc blende-type crystal structure.¹⁷⁾ Each atom is tetrahedrally surrounded by four atoms of the counterpart element, and, subsequently, Sb is in a configuration of cubic symmetry. In the GaSb and InSb matrices, ^{119}Sb atoms undoubtedly occupy the Sb site, and the emission line observed for the matrices is attributed to ^{119}Sn remaining at the Sb site on the basis of the above-described consideration of the recoil energy. The isomer shifts observed in the present work (GaSb 1.86 mm s⁻¹, InSb 1.94 mm s⁻¹) are in good agreement with those of ^{119}Sn arising from ^{119}Sb implanted at the Sb sites of GaSb and InSb.^{18,19)} The isomer shifts show that the ^{119}Sn atoms are covalently coordinated by four Ga or In atoms and that the s-electron density at the ^{119}Sn nuclei is only slightly smaller than that of ^{119}Sn in diamond-type α -tin (2.05 mm s⁻¹).²⁰⁾

The line of a sample with a nominal composition of In $^{119}\text{Sb}_{0.97}$ and the dominant one of the In $^{119}\text{Sb}_{1.03}$ are ascribed to ^{119}Sn in the InSb phase of the samples. The subsidiary peak of the latter sample is assigned to ^{119}Sn in the Sb metal phase. These observations are in contrast with those on SnTe in our previous study concerning the site distribution of ^{119}Sb , which revealed that most ^{119}Sb atoms occupy the Te site in $\text{SnTe}_{0.97}$, and that all of them occupy the Sn site in $\text{SnTe}_{1.03}$.⁵⁾ This difference is considered to originate due to the fact that the site of ^{119}Sn is determined by its parent ^{119}Sb , which has an intermediate nature between the two kinds of constituent atoms of the matrix, in the latter case of SnTe.

InSb($^{119\text{m}}\text{Te}$). For the InSb($^{119\text{m}}\text{Te}$) sample, the assignment of the lattice position of $^{119\text{m}}\text{Te}$ is not necessarily straightforward. In a previous paper we showed that the distribution of carrier-free ^{119}Sb and $^{119\text{m}}\text{Te}$ atoms between the two lattice sites of SnTe (see above) and SnSb upon solidification of the matrices is determined by the chemical nature of the atoms concerned.⁴⁾ It was also demonstrated that the fraction of ^{119}Sb displaced by the recoil associated with the EC decay of $^{119\text{m}}\text{Te}$ in $\text{Sn}^{119\text{m}}\text{Te}$ and $\text{Sb}_2^{119\text{m}}\text{Te}_3$ is in the range of

Table 1. Mössbauer Parameters of the Emission Lines of ^{119}Sn in the Compounds Labeled with ^{119}Sb and $^{119\text{m}}\text{Te}$

Source material	Isomer shift ^{a)} mm s^{-1}	Quadrupole splitting/ mm s^{-1}	Relative area	Line width mm s^{-1}	Lattice position of ^{119}Sn
Ga^{119}Sb	1.86 ± 0.03		100	1.12	Sb site
In^{119}Sb	1.94 ± 0.03		100	1.12	Sb site
$\text{In}^{119}\text{Sb}_{0.97}$	1.96 ± 0.03		100	1.15	Sb site
$\text{In}^{119}\text{Sb}_{1.03}$	1.97 ± 0.03		97	1.20	Sb site
	$2.68^{\text{b)}}$		3	$1.20^{\text{c)}}$	
$\text{InSb}(^{119\text{m}}\text{Te})$	1.88 ± 0.05		77	1.07	Sb site
	2.3 ± 0.1		23	1.2	In site
$\text{In}_2^{119\text{m}}\text{Te}_3$	3.21 ± 0.05		78	2.33	In site
	1.6 ± 0.3	1.5 ± 0.3	22	1.5	Te site
Zn^{119}Sb	2.05 ± 0.03	1.36 ± 0.03	100	1.15	Sb site
Cd^{119}Sb	2.10 ± 0.03	1.13 ± 0.03	100	1.18	Sb site
$\text{Cd}^{119\text{m}}\text{Te}$	2.36 ± 0.03	0.81 ± 0.03	100	1.53	Te site
$\text{Ag}_2^{119\text{m}}\text{Te}$	2.25 ± 0.03	2.32 ± 0.03	100	1.35	Te site

a) Relative to BaSnO_3 at liquid nitrogen temperature. b) Fixed in the fitting at the position for ^{119}Sn in Sb metal.²⁾ c) Assumed to be equal to that of the main peak.

12–22%.⁴⁾ When these empirical rules are applied to the case of $\text{InSb}(^{119\text{m}}\text{Te})$, its emission spectrum is reasonably interpreted as follows. The carrier-free $^{119\text{m}}\text{Te}$ atoms, being more electronegative than both of the constituent atoms of the matrix, occupy the site of the more electronegative component of the matrix, that is, the Sb site. The EC decay of $^{119\text{m}}\text{Te}$ results in a partial displacement of ^{119}Sn from the original site, giving two emission lines. The line with an isomer shift of 1.88 mm s^{-1} is ascribed to the ^{119}Sn remaining at the Sb site on the basis of the close similarity of the isomer shift with that of ^{119}Sn at the Sb site of In^{119}Sb described above as well as its dominance over the other line. The other line with an isomer shift of 2.3 mm s^{-1} is then assigned to ^{119}Sn arising from ^{119}Sb , which had been transferred to the In site or to an interstitial site, as a result of the EC decay of $^{119\text{m}}\text{Te}$. The isomer shift is in the range of those for normal and defect ^{119}Sn with nearest-neighbor Sb atoms (2.79 mm s^{-1} for SnSb and 2.30 mm s^{-1} for ^{119}Sn at the Te site in $\text{Sb}_2^{119\text{m}}\text{Te}_3$).⁴⁾ On the other hand, ^{119}Sn at the interstitial site in Si and α -tin is reported to have an isomer shift higher than that of ^{119}Sn at the substitutional site.^{15,21)} Therefore, ^{119}Sn atoms corresponding to the line at 2.3 mm s^{-1} are considered to be located at the In site rather than the interstitial one.

$\text{In}_2^{119\text{m}}\text{Te}_3$. In_2Te_3 has a unique zinc blende-type structure, in which the In positions are not entirely filled.¹⁷⁾ The dominant singlet observed for the $\text{In}_2^{119\text{m}}\text{Te}_3$ sample is assigned to ^{119}Sn displaced to the In site of the matrix, since its isomer shift (3.21 mm s^{-1}) is close to those of ^{119}Sn in SnTe (3.54 mm s^{-1})⁴⁾ and defect ^{119}Sn at the Sb site of $^{119}\text{Sb}_2\text{Te}_3$ (3.39 mm s^{-1}),²⁾ both having Te atoms as the nearest-neighbor atoms. The large line-width of the singlet suggests the presence of unresolved and probably distributed quadrupole

splitting ascribable to vacancies produced by the displacement of ^{119}Sb in the first, and possibly farther, coordination spheres of ^{119}Sn .

The doublet is then attributed to the ^{119}Sn remaining at the Te site on the basis of the isomer shift and quadrupole splitting. Namely, the low isomer shift (1.6 mm s^{-1}) suggests less electronegative ligands than tellurium atoms. The quadrupole splitting is ascribed to the presence of nearby vacancies at the In site. In the ordinary matrices studied so far, the relative area of the line due to ^{119}Sn displaced from the original site of $^{119\text{m}}\text{Te}$ was in the 12–22% range, as described above. However, in the present case of $\text{In}_2^{119\text{m}}\text{Te}_3$, the value is as high as 78%. This large value is reasonably interpreted in terms of the vacancies in the matrix. The minimum energy required to displace an atom in the direction of the vacancies is considered to be much lower than the displacement energy in normal solids. Moreover, the In site is considered to be more favorable for Sn atoms than the Te site because the chemical nature (electronegativity, valence etc.) of Sn is closer to that of In than that of Te. Sb_2Te_3 has a rhombohedral structure with no intrinsic vacancies, and the above discussion does not apply to $\text{Sb}_2^{119\text{m}}\text{Te}_3$.

It is reported that tin impurity atoms in In_2Te_3 ($\text{In}_2\text{Te}_3\text{Sn}_x$, $x=0.015$, 0.04 , and 0.08) gave a high isomer shift of 3.58 mm s^{-1} at room temperature, irrespective of the composition²²⁾ and in $\text{In}_2\text{Te}_3\text{Sn}_{0.02}$ gave 3.71 mm s^{-1} ,²³⁾ suggesting a configuration around ^{119}Sn different from that in our $\text{In}_2^{119\text{m}}\text{Te}_3$ sample. The tin impurity atoms in $\text{In}_2\text{Te}_3\text{Sn}_{0.02}$ were concluded to be at octahedral interstitials in the divalent state, forming chemical bonds with tellurium atoms on the basis of the closeness of the isomer shift to that of SnTe .

Mo et al. studied $^{119\text{m}}\text{Te}$ introduced in Ga_2Te_3 , which has the same crystal structure as In_2Te_3 .²⁴⁾ From a

crystallographic point of view, they assigned the two observed emission peaks with 'puzzling' isomer shifts to ^{119}Sn atoms at Te sites with different surroundings of Ga atoms and vacancies, not taking account of the displacement of ^{119}Sb due to the EC decay of $^{119\text{m}}\text{Te}$. Our assignment on $\text{In}_2^{119\text{m}}\text{Te}_3$ results in reasonable Mössbauer parameters as described above.

Zn ^{119}Sb and Cd ^{119}Sb . The structure of these compounds is a deformed diamond arrangement in which each atom is tetrahedrally surrounded by one of its own and three of the opposite kind of atoms.¹⁷⁾ The asymmetric configuration generates an electric-field gradient at each atom. The ^{119}Sn atom arising from ^{119}Sb is considered to remain at the original Sb site, being surrounded by one Sb atom and three Cd or Zn atoms. Therefore, the observed two lines are ascribed to a quadrupole doublet of ^{119}Sn at the Sb site of the matrices (Table 1).

Cd $^{119\text{m}}\text{Te}$. CdTe has the same zinc blende-type crystal structure as do InSb and GaSb.¹⁷⁾ Since the peak position (1.95 mm s^{-1}) of the more intense of the observed two lines is close to the isomer shift of ^{119}Sn at the Sb site in Cd ^{119}Sb , the line may be ascribed to ^{119}Sn arising from ^{119}Sb having remained at the Te site. However, the position of the other less intense line at 2.76 mm s^{-1} is too small to be ascribed to ^{119}Sn atoms at the Cd site, that is, ^{119}Sn having nearest-neighbor Te atoms (Table 1).

The Mössbauer emission spectrum of ^{119}Sn arising from $^{119\text{m}}\text{Cd}$ implanted into CdTe at 77 K was reported to exhibit a line with an isomer shift of 2.73 mm s^{-1} which was ascribed to Sn at the Cd site associated with a Te vacancy on the basis of the site-selective implantation mechanism and annealing behavior.²⁵⁾ The isomer shift is essentially identical with that of the less-intense line in our chemically prepared Cd $^{119\text{m}}\text{Te}$. However, the relative intensity of the line (47%) is too large to be ascribed to an ^{119}Sn being transferred to the Cd site from the Te site, compared with the corresponding values of 12–22% observed for InSb($^{119\text{m}}\text{Te}$), Sn $^{119\text{m}}\text{Te}$, and Sb $_2^{119\text{m}}\text{Te}_3$.⁴⁾

Our interpretation of the spectrum of Cd $^{119\text{m}}\text{Te}$ is that the two emission lines are a doublet due to ^{119}Sn at the Te site. ^{119}Sb atoms displaced from the Te site due to the recoil are considered in this case to have returned to the original Te site, because the Cd site, a site for electropositive ions in the matrix, is much less favorable for Sb. The isomer shift is slightly larger than that of ^{119}Sn in Cd ^{119}Sb . The small quadrupole splitting suggests nearby defects.

Ag $_2^{119\text{m}}\text{Te}$. The emission spectrum of ^{119}Sn in this sample comprised two lines with essentially the same intensity and width. The line at 3.41 mm s^{-1} alone may be ascribed to ^{119}Sn at the Ag site with the nearest-neighbor Te atoms because the line position is similar to the isomer shift of SnTe (3.54 mm s^{-1}). Then, however, an assignment of the other line becomes difficult,

its isomer shift (1.09 mm s^{-1}) being too small to be assigned to ^{119}Sn at the Te site with the nearest-neighbor Ag atoms or to ^{119}Sn at other possible sites. Moreover, it is not probable that the two different sites happen to have essentially equal widths and relative areas.

Thus, the observed two lines are ascribed to a quadrupole doublet (isomer shift 2.25 mm s^{-1} , quadrupole splitting 2.32 mm s^{-1}) of ^{119}Sn at the Te site in the monoclinic¹⁷⁾ Ag $_2\text{Te}$. The isomer shift (2.25 mm s^{-1}) is close to those of Ag $_3\text{Sn}$ (2.14 mm s^{-1})²⁰⁾ and ^{119}Sn arising from ^{119}Sb in Ag metal (2.10 mm s^{-1}).²⁶⁾ The Mössbauer spectrum of ^{125}Te revealed that Ag $_2\text{Te}$ is an ionic compound with 1.4 electrons on the tellurium atom,²⁷⁾ indicating that a negatively charged Te site is more favorable for ^{119}Sb atoms. All of the ^{119}Sb atoms arising from $^{119\text{m}}\text{Te}$ are considered to have been stabilized at the site of Te, rather than at the Ag site.

Systematics of the Isomer Shifts. Figure 6 shows the relationship between the isomer shifts of defect as well as normal ^{119}Sn atoms and the Pauling electronegativity of their nearest-neighbor atoms in binary compounds of antimony and tellurium with elements from silver through iodine. For ZnSb and CdSb, weighted averages of the electronegativities for two kinds of ligand atoms were employed. Starting from those compounds with the most electropositive gallium, the isomer shift is seen to increase along with an increase in the electronegativity of ligands.

A number of systematics have been reported on isomer shifts of ^{119}Sn in tin compounds.²⁸⁾ The correlation between the isomer shift of tetravalent tin and the electronegativity of the surrounding atoms has been discussed by a number of workers.²⁸⁾ Certain correlations between the isomer shifts of impurity tin in metals and the physical properties of matrices were also reported. The isomer shifts of impurity tin in pure metals were found to be inversely correlated with the effective force constant of the host matrix^{29,30)} as well as the electronegativity of the host metals.³¹⁾ The isomer shifts of tin in elemental semiconductors (α -Sn, Ge, and Si) were reported to increase along with an increase in the lattice constants of the host matrices.^{18,19)} Impurity Sn atoms at both the III and V sites of III–V compound semiconductors with low ionicity exhibited a trend similar to that found in the present work, while no such correlation was observed for Sn in compounds with high ionicity.¹⁹⁾ The present systematics shown in Fig. 6 is unique in that it comprises compounds of different structures, different coordination numbers and different types of bonding for both normal and defect ^{119}Sn . Since $\Delta R/R$ is positive for ^{119}Sn , the observed systematics indicates that the s-electron density at ^{119}Sn nucleus increases with an increase of the ligand electronegativity. This can be simply explained assuming a greater attraction of p-electrons by more electronegative ligands, resulting in less screening of s-electrons. However, our interpretation is that the systematics re-

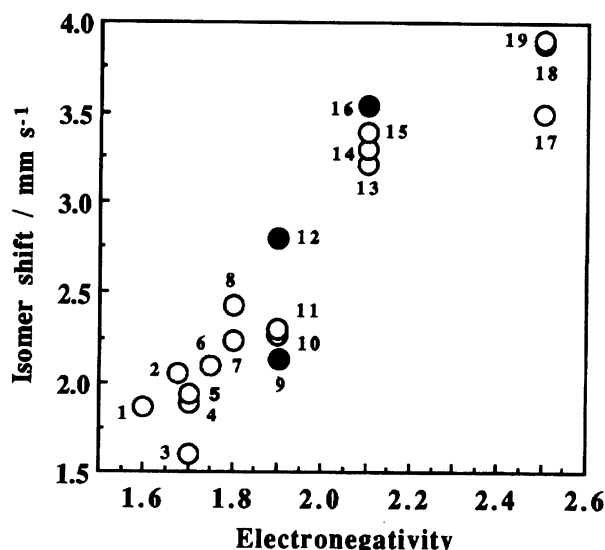


Fig. 6. Correlation between isomer shifts of defect and normal ^{119}Sn in binary compounds of antimony and tellurium with elements from silver through iodine and Pauling electronegativities of the nearest neighbor atoms. For ZnSb and CdSb , weighted averages of the electronegativities for two kinds of ligands were employed. Open circles refer to defect ^{119}Sn in Mössbauer emission measurements and closed ones to normal ^{119}Sn in Mössbauer absorption measurements. 1. Ga^{119}Sb (Sb site), 2. Zn^{119}Sb (Sb site), 3. $\text{In}_2^{119\text{m}}\text{Te}_3$ (Te site), 4. InSb ($^{119\text{m}}\text{Te}$) (Sb site), 5. In^{119}Sb (Sb site), 6. Cd^{119}Sb (Sb site), 7. $\text{Sn}^{119\text{m}}\text{Te}$ (Te site),⁴⁾ 8. Sn^{119}Sb (Sb site),⁴⁾ 9. Ag_3Sn ,²⁰⁾ 10. $\text{Ag}_2^{119\text{m}}\text{Te}$ (Te site), 11. $\text{Sb}_2^{119\text{m}}\text{Te}_3$ (Te site)²⁾ and InSb ($^{119\text{m}}\text{Te}$) (In site), 12. SnSb ,⁴⁾ 13. $\text{Sb}_2^{119\text{m}}\text{Te}_3$ (Sb site),⁴⁾ and $\text{In}_2^{119\text{m}}\text{Te}_3$ (In site), 14. $\text{Sn}^{119\text{m}}\text{Te}$ (Sn site),⁴⁾ 15. $^{119}\text{Sb}_2\text{Te}_3$ (Sb site),²⁾ 16. SnTe ,⁴⁾ 17. $^{119\text{m}}\text{TeI}_4$ (Sn(II), Te site),³⁾ 18. SnI_2 ,²⁰⁾ 19. $^{119}\text{SbI}_3$ (Sb site).³⁾

fects a gradual variation of character of the bonding from a metallic one, for which the effective number of s-electrons is approximately one, to the s^2 -type one.

The authors are thankful to the former staff of the Riken 160 cm cyclotron for many irradiation runs and also to Mr. Y. Iimura for X-ray powder pattern measurement.

References

- 1) D. L. Nagy, *Hyperfine Interact.*, **83**, 3 (1994), and the literature cited therein.
- 2) F. Ambe, S. Ambe, H. Shoji, and N. Saito, *J. Chem. Phys.*, **60**, 3773 (1974).
- 3) F. Ambe and S. Ambe, *Bull. Chem. Soc. Jpn.*, **47**, 2875 (1974).
- 4) F. Ambe and S. Ambe, *J. Chem. Phys.*, **73**, 2029 (1980).
- 5) F. Ambe and S. Ambe, *J. Chem. Phys.*, **75**, 2463 (1981).
- 6) T. Okada, S. Ambe, F. Ambe, and H. Sekizawa, *J. Chem. Phys.*, **86**, 4726 (1982).
- 7) F. Ambe, S. Ambe, T. Okada, and H. Sekizawa, "Geochemical Processes at Mineral Surfaces (ACS Symposium Series 323)," ed by J. A. Davis and K. F. Hayes, American Chemical Society, Washington, D. C. (1986), p. 403.
- 8) S. Ambe and F. Ambe, *Bull. Chem. Soc. Jpn.*, **63**, 3260 (1990).
- 9) S. Ambe and F. Ambe, *Bull. Chem. Soc. Jpn.*, **64**, 1289 (1991).
- 10) G. Stevens and Y. Zhang, "Ion Implantation Handbook," Mössbauer Effect Data Center, Asheville (1988).
- 11) G. Weyer, *Nucl. Instr. Methods*, **186**, 201 (1981).
- 12) G. Weyer, *Hyperfine Interact.*, **27**, 249 (1986).
- 13) H. de Waard and L. Niesen, "Mössbauer Spectroscopy Applied to Inorganic Chemistry," ed by G. J. Long, Plenum, New York (1987), Vol. 2, p. 1.
- 14) H. de Waard, *Hyperfine Interact.*, **72**, 229 (1992).
- 15) A. Nylandsted Larsen, G. Weyer, and L. Nanver, *Phys. Rev. B*, **B21**, 4951 (1980).
- 16) G. L. Zhang, D. Mo, Z. N. Liang, and L. Niesen, *Hyperfine Interact.*, **56**, 1661 (1990).
- 17) R. W. G. Wyckoff, "Crystal Structure," 2nd ed, Interscience, New York (1963), Vols. 1 and 2.
- 18) G. Weyer, J. W. Petersen, S. Damgaard, H. L. Nielsen, and J. Heinemeier, *Phys. Rev. Lett.*, **44**, 155 (1980).
- 19) G. Weyer, J. W. Petersen, and S. Damgaard, *Physica B+C*, **116B**, 470 (1983).
- 20) J. Silver, C. A. Mackay, and J. D. Donaldson, *J. Mater. Sci.*, **11**, 836 (1976).
- 21) G. Weyer, J. W. Petersen, and S. Damgaard, *Hyperfine Interact.*, **10**, 775 (1981).
- 22) V. M. Koshkin, E. E. Ovechkina, and V. P. Romanov, *Sov. Phys. JETP (Engl. Transl.)*, **42**, 1128 (1976).
- 23) F. S. Nasredinov, V. F. Masterov, Ch. S. Saidov, P. P. Seregin, N. N. Troitskaya, and H. U. Tschirner, *Phys. Status Solidi, A*, **107**, 291 (1988).
- 24) D. Mo, G. L. Zhang, Z. N. Liang, and L. Niesen, *Hyperfine Interact.*, **56**, 1621 (1990).
- 25) H. Grann, F. T. Pedersen, and G. Weyer, *Hyperfine Interact.*, **29**, 1237 (1986).
- 26) H. Andreasen, S. Damgaard, H. L. Nielsen, J. W. Petersen, and G. Weyer, *Hyperfine Interact.*, **23**, 43 (1985).
- 27) H. Sakai, M. Ando, and Y. Maeda, *Hyperfine Interact.*, **68**, 201 (1991).
- 28) P. A. Flinn, in "Mössbauer Isomer Shifts," ed by G. K. Shenoy and F. E. Wagner, North-Holland, Amsterdam (1978), p. 592.
- 29) V. A. Bryukhanov, N. N. Delyagin, and V. S. Shpinel', *Sov. Phys. JETP (Engl. Transl.)*, **20**, 55 (1965).
- 30) J. W. Petersen, O. H. Nielsen, G. Weyer, E. Antoncik, and S. Damgaard, *Phys. Rev. B*, **B21**, 4292 (1980).
- 31) N. N. Delyagin and V. I. Nesterov, *Sov. Phys. JETP (Engl. Transl.)*, **64**, 1367 (1986).